Applied Radiation and Isotopes 107 (2016) 299–311

Contents lists available at ScienceDirect

Applied Radiation and Isotopes

journal homepage: www.elsevier.com/locate/apradiso

"Hot background" of the mobile inelastic neutron scattering system for soil carbon analysis

Aleksandr Kavetskiy, Galina Yakubova *, Stephen A. Prior, H. Allen Torbert

USDA-ARS National Soil Dynamics Laboratory, 411 South Donahue Drive, Auburn, AL 36832, United States

HIGHLIGHTS

- Neutron activated "hot background" of Al, Fe, Si, SiO_2, NG MP320 was investigated.
- Activated isotopes and γ-peaks were identified.
- Activated isotopes in soil and MINS construction materials were listed.
- Contribution of hot background should be accounted in soil carbon analysis.

ARTICLE INFO

Article history:
Received 12 May 2015
Received in revised form
23 October 2015
Accepted 5 November 2015
Available online 6 November 2015

Keywords:
Neutron activation
Hot background
Neutron generator
Soil carbon analysis
Radioisotopes ^{28}Al, ^{56}Mn, ^{27}Mg, ^{24}Na, ^{16}N

ABSTRACT

The problem of gamma spectrum peak identification arises when conducting soil carbon analysis using the inelastic neutron scattering (INS) system. Some spectral peaks could be associated with radioisotopes appearing due to neutron activation of both the measurement system and soil samples. The investigation of "hot background" gamma spectra from the construction materials, whole measurement system, and soil samples over time showed that activation of ^{28}Al isotope can contribute noticeable additions to the soil neutron stimulated gamma spectra.

1. Introduction

The method of gamma response measurement from soil due to inelastic neutron scattering (INS) was applied for determining soil carbon content. Different aspects of this method, which has a number of advantages over other methods of soil carbon determination, have been discussed to date. The theoretical background of this method, construction of measurement equipment, operational guidelines and data processing, radiation safety requirements, and results of routine field testing were described and published in a number of reports and articles (e.g., Wielopolski et al., 2004; Wielopolski, 2011; Yakubova et al., 2014). In spite of that, some important issues were not considered in these earlier publications.

The problem of gamma spectrum peak identification arises when conducting soil carbon (and other elements) analysis using the INS system. The peaks in the INS gamma spectra appear mainly due to INS and thermal neutron capture (TNC) processes with nuclei of elements present in the equipment and soil samples, but some peaks may be associated with radioisotopes that appear from neutron irradiation (delay activation, DA) of all components of the measurement system (neutron generator, gamma detector, construction materials) and soil samples. The gamma radiation from DA adds not only to the INS spectra, but also to the natural background spectra when neutron irradiation is off (so called "hot background"), while the INS and TNC gamma rays disappear. The "hot background" decreases with time according to the half-life of the created isotopes and can be studied using these dependencies. Analysis of the "hot background" gamma spectra of materials of interest and measurement equipment, and the addition to INS spectra are discussed in this article.

Radioactive isotopes appear due to the nuclear reaction of neutrons with nuclei in the irradiated objects (i.e., the neutron activation process). These nuclear reactions (activation) can occur due to both the interaction of fast neutrons (in the MeV energy range) with nuclei [e.g., reactions (n,p), (n,α), (n,d), (n,t), etc.], and the interaction of thermal neutrons with nuclei in the neutron capture process. The isotopes produced are usually radioactive and

* Corresponding author. Fax: (334) 887-8597.
E-mail address: galina.yakubova@ars.usda.gov (G. Yakubova).

http://dx.doi.org/10.1016/j.apradiso.2015.11.012
0969-8043/

their decay can be accompanied by a γ-quantum issue. The activity of activated isotopes per unit volume ($A_{act,i}$, Bq cm^{-3}) depends on neutron flux intensity (φ, cm^{-2} s^{-1}), concentration of the parent nucleus (N, cm^{-3}), cross section of the neutron-parent nucleus interaction (σ, cm^2), decay time constant of the produced nucleus (λ_i, s^{-1}), and the irradiation time (t_{irr}, s); this can be calculated by Eq. (1) (Turner, 2007):

$$A_{act,i}(t_{irr}) = N \bullet \sigma \bullet \phi \bullet [1 - \exp(-\lambda_i \bullet t_{irr})] \quad (1)$$

Eq. (1) illustrates that if the irradiation time is much greater (at least 3–4 times) than the half-life ($T_{1/2}=0.693/\lambda$) of the isotope, the activity reaches a constant level regardless of further irradiation. With an irradiation time much less than the isotope half-life, the increase in isotope activity is approximately directly proportional to irradiation time. The γ-quanta of activated isotopes will contribute to the gamma spectra when carrying out soil carbon analysis with the MINS system. The gamma spectra for the MINS system components and soil samples immediately following irradiation (i.e., "hot background", gamma spectra measured directly after neutron activation) when the neutron flux is off, consists of gamma rays from isotopes spawned from activation and will degrade with time (according to radioactive decay law) to natural background levels. The effect of gamma radiation from activated isotopes can be understood and estimated by measuring the "hot background" spectra over time, determining the set of peaks and count rate for each at time zero, and comparing this with the count rate in the appropriate energy range of the MINS system spectra. Thus, the contribution of the "hot background" (or "delay activation") to the MINS system spectra of the studied object can be determined.

For an accurate assessment of soil carbon, it is important to account for the "hot background" spectra and their evolution with time. The goal of the present work was to examine the MINS system as a whole, its components, and its construction materials to determine appropriate "hot background" values for proper analysis of spectra peaks over time, to identify the activated radioisotopes responsible for gamma peaks, and to estimate the effect of activated isotopes on the recorded MINS spectra for the measured object.

2. Materials and methods

To determine the studied object's "hot background" spectrum, it should be irradiated by neutrons; immediately following irradiation, the object is quickly moved to a non-activated area where the gamma spectra measurement is initiated. The gamma detector and other associated equipment used for measurement should also be non-activated. The acquired spectra will represent the sum of the "hot background" spectra of the studied object and the natural background for the place of measurement. Therefore, the natural background spectrum should have been previously determined for this location.

The natural background spectra is created by radioisotopes emitting gamma quanta at a constant rate, and the appropriate j-th peak in the spectra increases directly proportional to the acquisition time. The radioisotopes forming the "hot background" spectra of the studied object decay and issue gamma quanta according to the radioactive decay law; increase of the appropriate j-th peak in the spectra slows down with acquisition time according to the same law. The spectra are recorded throughout the time interval. The difference between the sequentially recorded spectra divided by the time interval between their recordings gives the gamma rate spectrum at a moment approximately corresponding to the middle of the time interval. The intensity of these spectra will decrease over time and approach the natural background spectrum (in counts per second, cps) and finally coincide with it. At the beginning (time moment at the end of irradiation), the "hot background" is the part of the spectra measured at irradiation due to activated isotopes ("delay activation spectrum"). The dependence of the count rate in j-th channel (at j-th energy) with time, $Y_j(t)$, is determined by decay of the isotope's emitted gamma quanta with this energy and can be described by Eq. (2):

$$Y_j(t) = \sum_i G_{i,j} \bullet \exp(-\lambda_i \bullet t) + B_j \quad (2)$$

where $G_{i,j}$ is the gamma flux on the detector surface which is the i-th isotope with energy in j-th channel at the end of the irradiation produces; and B_j is the intensity of the natural background in j-th channel. The decay time constants can be determined by approximating experimental dependencies using Eq. (2). Such approximation can be done using standard software such as IGOR (WaveMetrics, 2013). Note that B_j parameter is known from the natural background measurement and should be fixed. Comparison of the determined decay time constants and peak centroid energy with reference data allows for the identification of the isotopes responsible for this peak (i.e., within the bounds of measurement and approximation accuracy).

The "hot background" spectra from the MINS system as a whole and from the neutron generator, gamma detector NaI(Tl), aluminum and steel construction components of the system were studied. At the beginning of the investigation, massive pieces of aluminum and steel were irradiated by neutrons and their "hot background" spectra were studied. Since silicon dioxide is a major component of soil, the "hot background" of silicon dioxide and silicon were also evaluated. Based on these investigations, the addition of all "hot backgrounds" to the MINS spectra was estimated. The origin of the peaks in "hot background" for the MINS (whole system, components and materials) were identified. The results of these investigations are reported here.

3. Results and discussion

3.1. Aluminum "hot background"

Aluminum is the primary material used in the MINS system construction. To determine the "hot background" spectra from this material, a 50 cm × 50 cm × 10 cm aluminum block was irradiated for 1 h with neutrons by placing the neutron generator (Model MP320; Thermo Fisher Scientific, Colorado Springs, CO; 14 MeV, total flux 10^7 neutron per second) directly on the block.

After irradiation, the aluminum block was moved to a non-irradiated area and the "hot background" spectra was acquired over several days using a non-irradiated NaI(Tl) gamma detector; 32 intermediate spectra were recorded on the computer during that time. The channel by channel difference between two sequentially recorded spectra divided by the time between their recordings were calculated. Each calculated spectrum is the aluminum "hot background" spectrum (in cps per channel) at the time corresponding to the middle of the recording interval; this and the previously determined natural background spectrum are shown in Fig. 1. As seen in the 300–5500 keV energy range, the "hot background" spectra exceeded the natural background and contained several additional peaks which are absent in the natural background. All of these peaks disappear with time at varying rates until the "hot background" spectra reached the level of natural background.

The time dependence of spectra intensity, mainly at points coinciding with peak centroids, were plotted to determine the law and time constant of spectral decrease (Fig. 2). All of these can be

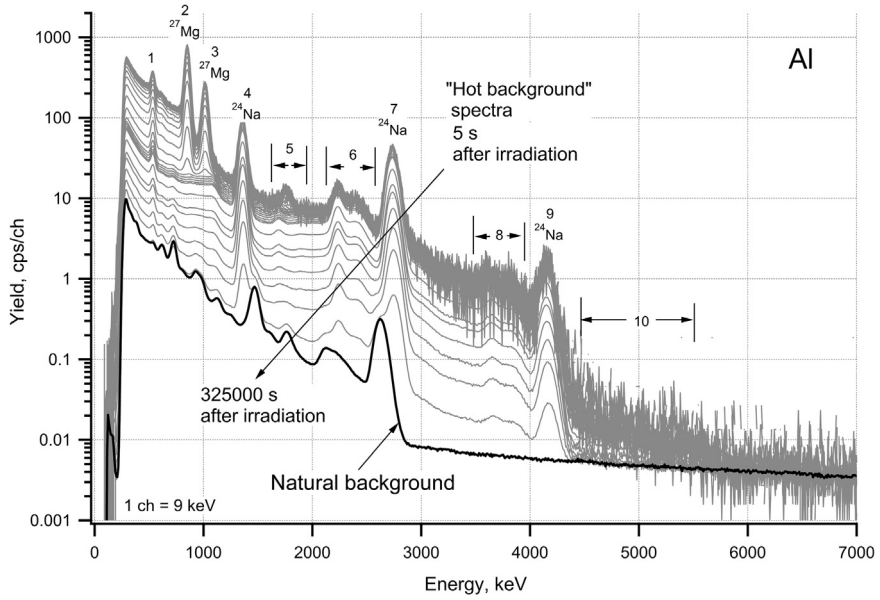

Fig. 1. Aluminum block "hot background" spectra at different times following neutron irradiation, and the natural background spectrum. For numbers on plots (i.e., peak or areas numbers) see Table 1. Main isotopes associated with some peaks are shown near the peaks.

approximated by the radioactive decay law with one or two exponential terms; a constant portion agrees with natural background spectrum at selected points (energies) in the spectra. These radioactive decay law approximations are shown in Fig. 2 by solid lines and are in good agreement with experimental results. The time constants used in fits agreed with reference data (NNDC, 2012) for isotopes emitting gamma quanta with energy equal to those of peak centroids. Note that the dependencies for 1368 keV (peak 4), 2754 keV (peak 7) and 4122 keV (peak 9) energies can be approximated by Eq. (2) using one exponential term with a time constant of $1.28 \cdot 10^{-5}\ s^{-1}$. Based on peaks position and time constants, the above listed three peaks can be attributed to isotope ^{24}Na. This isotope can appear due to the ^{27}Al(n,α)^{24}Na reaction. The dependencies for 844 keV (peak 2), and 1014 keV (peak 3) energies can be approximated using two exponential terms with time constants of $1.22 \cdot 10^{-3}\ s^{-1}$ and $1.28 \cdot 10^{-5}\ s^{-1}$. The first term can be attributed to the isotope ^{27}Mg which can appear due to the ^{27}Al(n,p)^{27}Mg reaction. The second term in the 1014 keV peak can be attributed to Compton scattering (CS) from the 1368 keV peak of ^{24}Na. The dependence for 1780 keV energy (i.e., 5 peak, Fig. 2) can be approximated using two exponential terms with time constants of $5.16 \cdot 10^{-3}\ s^{-1}$ and $1.28 \cdot 10^{-5}\ s^{-1}$. The first term can be attributed to isotope ^{28}Al which appears due to the ^{27}Al($n_{thermal}$)^{28}Al reaction. The second term can be attributed to the double escape (DE) peak from 2754 keV of ^{24}Na (DE peak from energy 2754 keV is 1732 keV). Information about the processes and isotopes responsible for gamma peaks in the above mentioned and other areas of the aluminum "hot background" spectra, and

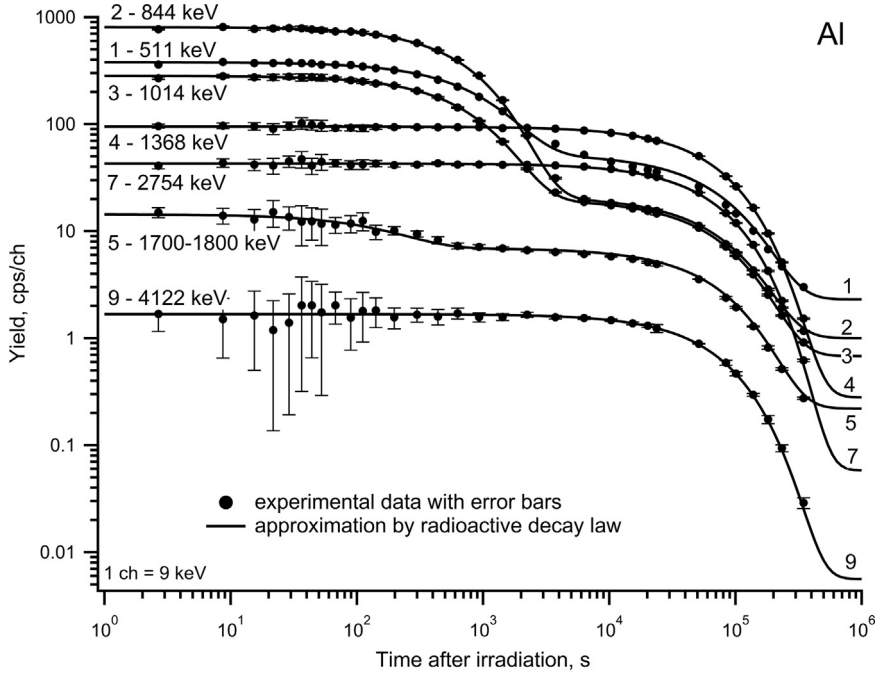

Fig. 2. Time dependencies of peaks in the aluminum "hot background" spectra. Integer 1–9 correspond to peak or area numbers in Fig. 1. Peak centroid positions are also shown for each curve.

Table 1
Positions and decreasing time constants of peaks in the aluminum "hot background" spectra, isotope and processes responsible for the peaks, and nuclear reaction producing the isotope.

Peak or area #	Peak centroid or energy range, keV	Time dependent fitting parameters		Isotope and $T_{1/2}$	Nuclear reaction producing the isotope	Process responsible for the peak
		Term #	Time constant, s^{-1}			
1	511	1	$0.99 \cdot 10^{-3}$	Unidentified		
		2	$1.28 \cdot 10^{-5}$	^{24}Na 15.0 h	^{27}Al(n,α)^{24}Na	Pair production peak of ^{24}Na gamma rays
2	844	1	$1.22 \cdot 10^{-3}$	^{27}Mg 9.46 m	^{27}Al(n,p)^{27}Mg	$^{27}Mg(\beta^-)^{27}Al^* \rightarrow {}^{27}Al+\gamma$
		2	$1.28 \cdot 10^{-5}$	^{24}Na 15.0 h	^{27}Al(n,α)^{24}Na	CS from 1368 keV
3	1014	1	$1.22 \cdot 10^{-3}$	^{27}Mg 9.46 m	^{27}Al(n,p)^{27}Mg	$^{27}Mg(\beta^-)^{27}Al^* \rightarrow {}^{27}Al+\gamma$
		2	$1.28 \cdot 10^{-5}$	^{24}Na 15.0 h	^{27}Al(n,α)^{24}Na	CS from 1368 keV
4	1368	1	$1.28 \cdot 10^{-5}$	^{24}Na 15.0 h	^{27}Al(n,α)^{24}Na	$^{24}Na(\beta^-)^{24}Mg^* \rightarrow {}^{24}Mg+\gamma$
5	1700–1800	1[a]	$5.16 \cdot 10^{-3}$	^{28}Al 2.28 m	$^{27}Al(n_{therm})^{28}Al$	$^{28}Al(\beta^-)^{28}Si^* \rightarrow {}^{28}Si+\gamma$
		2[b]	$1.28 \cdot 10^{-5}$	^{24}Na 15.0 h	^{27}Al(n,α)^{24}Na	DE from 2754 keV
6	2130–2590	Unidentified				
7	2754	1	$1.28 \cdot 10^{-5}$	^{24}Na 15.0 h	^{27}Al(n,α)^{24}Na	$^{24}Na(\beta^-)^{24}Mg^* \rightarrow {}^{24}Mg+\gamma$
8	3530–3960	Unidentified				
9	4122	1	$1.28 \cdot 10^{-5}$	^{24}Na 15.0 h	^{27}Al(n,α)^{24}Na	Coincidence 1368+2754 keV
10	4500–5500	Unidentified				

CS=Compton Scattering; SE=single escape; DE=double escape.
[a] Peak centroid 1780 keV.
[b] Peak centroid 1732 keV.

their time constants used in line fittings are shown in Table 1.

The isotopes ^{27}Mg[^{27}Al(n,p)^{27}Mg reaction] and ^{24}Na[^{27}Al(n,α)^{24}Na] are produced when aluminum is irradiated with fast neutrons. Moderation of fast neutron forms the thermal neutron flux. The isotope ^{28}Al can appear due to thermal neutron capture by ^{27}Al nuclei. Gamma radiation from decay of this isotope appears in the spectra. Gamma radiation which appear due to decay of the above listed isotopes should be accounted for in MINS measurements.

3.2. Iron "hot background"

Since iron is the chief component of the steel material used in construction of the MINS system, the "hot background" spectrum of this material was investigated. A 70 cm × 50 cm × 15 cm steel block was neutron irradiated for 1 h by the same MP320 generator placed directly on the block. After irradiation, the block was moved to a non-irradiated area and the "hot background" spectra was acquired over several days using a non-irradiated NaI(Tl) gamma detector. The "hot background" spectra (in cps) were

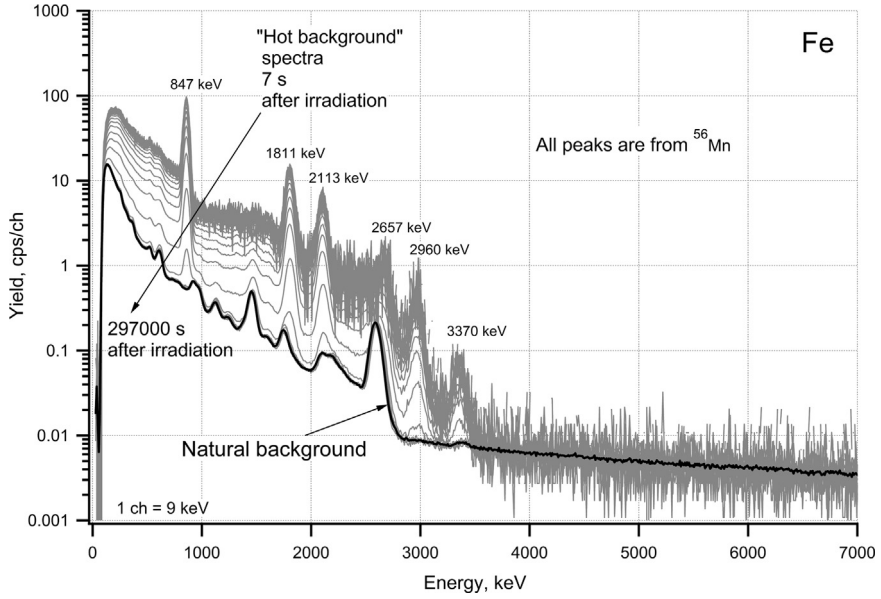

Fig. 3. Iron block "hot background" spectra for different times following neutron irradiation, and the natural background spectrum.

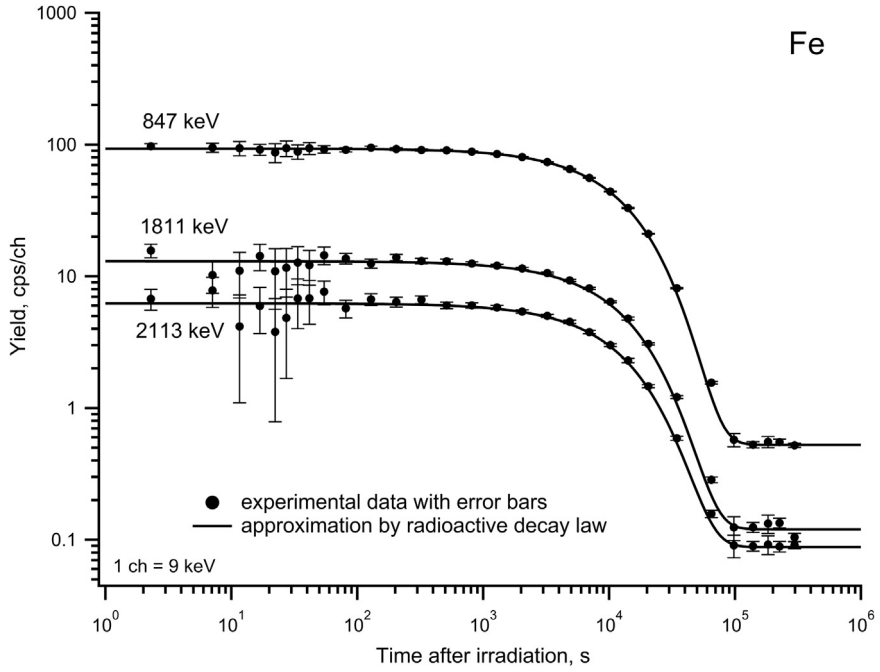

Fig. 4. Time dependencies of peaks in the iron "hot background" spectra. Peak centroid positions are shown for each curve.

calculated as described above for aluminum. These spectra and the natural background spectrum are shown in Fig. 3.

In this case, the series of the peaks with centroids at 847, 1811, 2113, 2657, 2960, and 3370 keV were observed. The time dependencies for the dominant peaks at 847, 1811, and 2113 keV are represented by point symbols in Fig. 4. Their approximation according to the radioactive decay law with one exponential term and a time constant of $7.54 \cdot 10^{-5}\ s^{-1}$ is shown in this figure and agrees well with experimental data. The above listed peak set is due to the isotope ^{56}Mn (NNDC, 2012.). The production of this isotope under neutron irradiation of the block can occur due to the ^{56}Fe(n,p)^{56}Mn reaction. The beta decay of this isotope yields the isotope ^{56}Fe and is accompanied by the emission of the above listed gamma lines. Therefore, ^{56}Mn gamma lines should be taken into account during MINS measurements. Information about the processes and isotopes responsible for gamma lines in the iron "hot background" spectra is given in Table 2.

3.3. Silicon "hot background"

Silicon content in soil varies between ~20 and 50 percent by weight (Wielopolski et al., 2005; Frank and Tolgyessy, 1993). Therefore, measurement of its "hot background" is important for determining possible additions of delay activated gamma lines to the MINS spectra. To conduct these measurements, granulated silicon with a bulk density of 1.2 g cm^{-3} and an average particle size of 0.5 cm was used. Fifty kilograms of silicon was neutron irradiated for 1 h by the MP320 generator that was placed directly on top of the material. After irradiation, the silicon was carefully moved (to avoid mixing) to a non-irradiated area and the "hot background" spectra was acquired over several days using a non-irradiated NaI(Tl) gamma detector. The spectra were processed as described above. The silicon "hot background" spectra along with the natural background spectra are shown in Fig. 5. These spectra have a dominant peak with a centroid at 1780 keV, low intensity peaks with centroids at 844, 1014, and 1273 keV, and some increased count rates in areas near 2400, 3000–3500 keV relative to the natural background spectrum.

The experimental count rates over time for the 1780, 1273 and 844 keV energies are shown in Fig. 6 by point symbols. Approximations of the dependencies according to the radioactive decay law with one exponential term having a time constant of $5.16 \cdot 10^{-3}\ s^{-1}$ for 1780 keV and with two exponential terms having time constants of $5.16 \cdot 10^{-3}\ s^{-1}$ and $1.76 \cdot 10^{-3}\ s^{-1}$ for 1273 keV are shown in Fig. 6 by lines. As can be seen the agreement is good. Based on data regarding peaks centroid and their time constants, the isotopes responsible for these peaks were identified. The 1780 keV peak was produced by ^{28}Al which appears due to the ^{28}Si(n,p)^{28}Al reaction. Its beta decay yields the isotope ^{28}Si with a concurrent 1780 keV gamma quantum emission. Counts at 1273 keV are the sum of CS from 1780 keV and gamma quanta from isotope ^{29}Al (from the ^{29}Si(n,p)^{29}Al reaction). Note

Table 2
Positions and decreasing time constants of peaks in the iron "hot background" spectra, isotope and processes responsible for the peaks, and nuclear reaction producing the isotope.

Peak centroid, keV	Time dependent fitting parameters		Isotope and $T_{1/2}$	Nuclear reaction producing the isotope	Process responsible for the peak
	Term #	Time constant, s^{-1}			
847	1	$7.54 \cdot 10^{-5}$	^{56}Mn	^{56}Fe(n,p)^{56}Mn	^{56}Mn(β$^-$)^{56}Fe*→^{56}Fe+γ
1811	1				
2113	1				
2657	Unidentified		2.58 h		
2960	Unidentified				
3370	Unidentified				

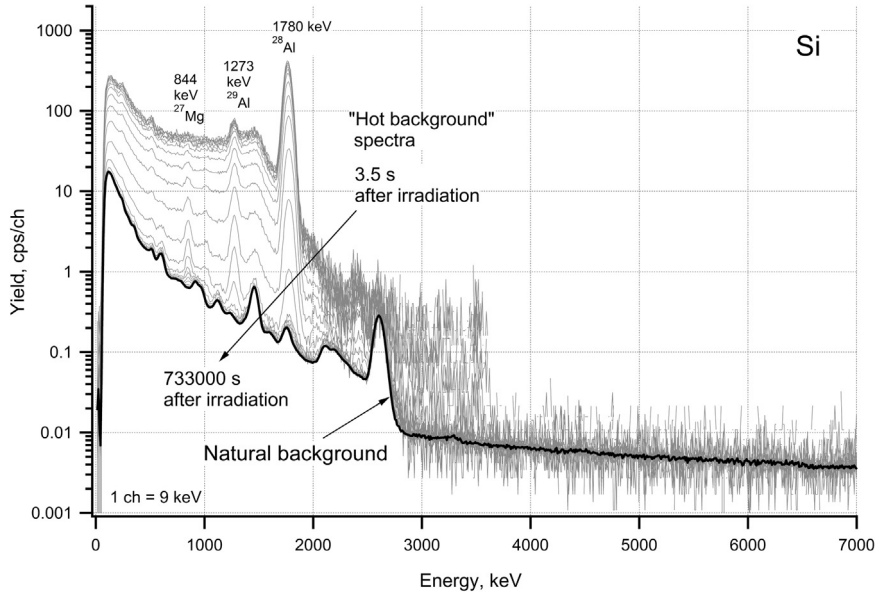

Fig. 5. Silicon "hot background" spectra for different times following neutron irradiation, and the natural background spectrum. Main isotopes associated with some peaks are shown near the peaks.

that the natural abundance of ^{29}Si is 4.67% (Wolfram Research, Inc. Champaign, IL). The ^{29}Al beta decay with a time constant of $1.76 \cdot 10^{-3}$ s^{-1} yields ^{29}Si and is accompanied by the issue of 1273 keV gamma quantum with a 91% intensity (NNDC, 2012).

In addition, gamma lines at 844 and 1014 keV in the silicon "hot background" spectra can be attributed to the ^{27}Mg isotope which may be produced by the reaction (n,α) on ^{30}Si [natural abundance 3% (Wolfram Research, Inc. Champaign, IL). The ^{27}Mg decay with a time constant of $1.22 \cdot 10^{-3}$ s^{-1} for 844 keV is shown in Fig. 6.

Thus, the gamma lines of the silicon hot background spectra (primarily the 1780 keV line), should be accounted for in the MINS measurements. Information about the processes and isotopes responsible for gamma lines in the silicon "hot background" spectra are given in Table 3.

3.4. Sand "hot background"

The "hot background" of sand (silicon dioxide) was investigated since it is usually a major component of soil. A 150 cm × 150 cm × 60 cm sand pit was used for this purpose. The neutron generator was placed directly on the sand surface in the middle of the pit. Irradiation by 14 MeV neutrons (total flux 10^7 neutron per second) was conducted for 1 h. After this, the neutron generator was removed, and a gamma detector was installed in its place. Recording of the "hot background" spectra was started immediately following the irradiation (delay no longer than 10 s).

The "hot background" spectra were processed as described above; these spectra along with the natural background spectra are shown in Fig. 7. The shape of the spectra up to 4000 keV is very similar to the silicon "hot background" spectra (Fig. 6); both

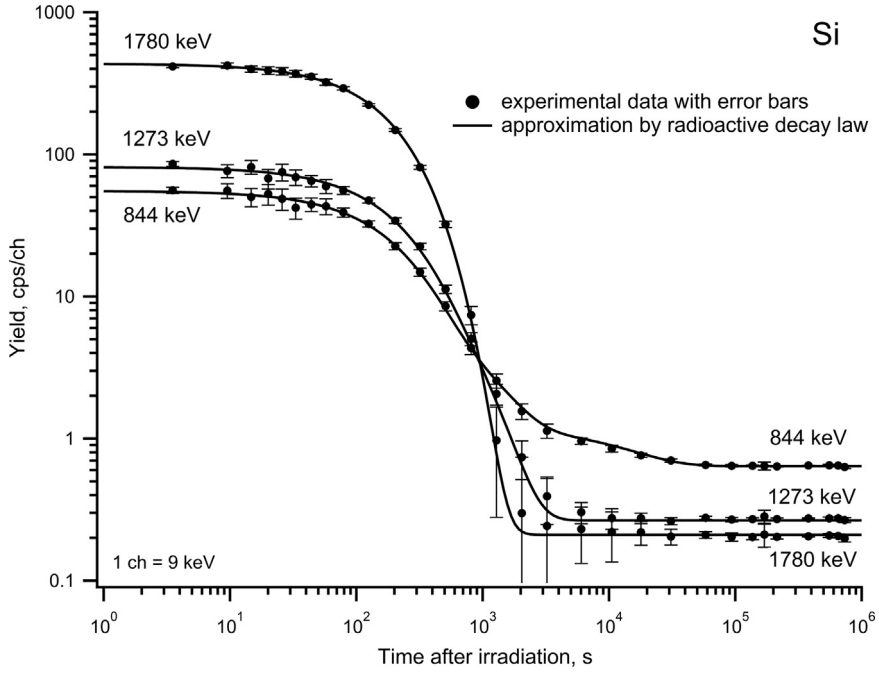

Fig. 6. Time dependencies of peaks in the silicon "hot background" spectra Peak centroid positions are shown for each curve.

Table 3
Positions and decreasing time constants of peaks in the silicon "hot background" spectra, isotope and processes responsible for the peaks, and nuclear reaction producing the isotope.

Peak centroid, keV	Time dependent fitting parameters		Isotope and $T_{1/2}$	Nuclear reaction producing the isotope	Process responsible for the peak
	Term #	Time constant, s^{-1}			
844	1	$1.22 \cdot 10^{-3}$	^{27}Mg 9.458 m	^{30}Si(n,α)^{27}Mg	^{27}Mg(β$^-$)^{27}Al*→^{27}Al+γ
	2	$5.16 \cdot 10^{-3}$	^{28}Al 2.28 m	^{28}Si(n,p)^{28}Al	CS from 1780 keV
1273	1	$1.76 \cdot 10^{-3}$	^{29}Al 6.56 m	^{29}Si(n,p)^{29}Al	^{29}Al(β$^-$)^{29}Si*→^{29}Si+γ
	2	$5.16 \cdot 10^{-3}$	^{28}Al 2.28 m	^{28}Si(n,p)^{28}Al	CS from 1780 keV
1780	1	$5.16 \cdot 10^{-3}$	^{28}Al 2.28 m	^{28}Si(n,p)^{28}Al	^{28}Al(β$^-$)^{28}Si*→^{28}Si+γ

CS=Compton Scattering.

displayed the same set of peaks and behavior over time (Fig. 8). Several additional low intensity peaks are present at higher energies compared to the silicon spectra. Obviously, these peaks are associated with oxygen. Three peaks with centroids around 6130, 5620, and 5110 keV were observed.

The experimentally measured count rate over time for the peak with a centroid at 6130 keV is shown in Fig. 8 (points with error bars). Despite the low intensity and relatively high count rate error, this dependence can be approximated by radioactive decay law with one exponential term at a time constant equal to 0.097 s^{-1} and agrees well with experimental data (within experimental error). Based on this, the peak can be attributed to the N16 isotope. These nuclei can appear due to the ^{16}O16(n,p)^{16}N nuclear reaction on oxygen in sand. Due to the ^{16}N beta decay, ^{16}O in the excited state appears. These excited nuclei fall to ground state with an emission of 6130 keV gamma quanta. The peaks with centroids around 5620 and 5110 keV can be attributed to the single escape (SE) and DE of the 6130 keV peak (6130–511 keV and 6130–1022 keV), respectively. Information about the processes and isotopes responsible for gamma lines in the sand "hot background" spectra are given in Table 4. Therefore, the gamma lines in the sand "hot background" spectra (primarily the 1780 keV line) should be accounted for in the neutron stimulated gamma spectra of sand.

3.5. Gamma detector "hot background"

The MINS system contains three NaI(Tl) gamma detectors with crystals, each measuring 12.7 cm × 12.7 cm × 15.2 cm. Each detector is contained within a double walled box composed of steel (inner wall) and aluminum (outer wall). For "hot background" measurement, the detector was neutron irradiated for 1 h with a MP320 generator placed directly on the detector. After irradiation, the detector was moved to a non-irradiated area and the "hot background" spectra was acquired over several days using a non-irradiated NaI(Tl) gamma detector. The detector's "hot background" spectra (and natural background spectrum) are shown in Fig. 9. Peaks with centroids at 1780 keV and 847 keV can be observed in these spectra. The time dependencies of counts rates for these energies are illustrated in Fig. 10 by point symbols. Radioactive decay law with two exponential terms was used for characterization of these dependencies. As can be seen, the approximation lines are in agreement with experimental observations within experimental error limits. Time constants for both cases are $5.16 \cdot 10^{-3}$ s^{-1} and $7.54 \cdot 10^{-5}$ s^{-1}, respectively. Taking these facts into account, the gamma line at 1780 keV can be attributed to the ^{28}Al and ^{56}Mn (1810 keV gamma line) isotopes, whereas the gamma line at 847 keV can be attributed to CS gamma rays from 1780 keV of ^{28}Al and ^{56}Mn isotopes. The reactions

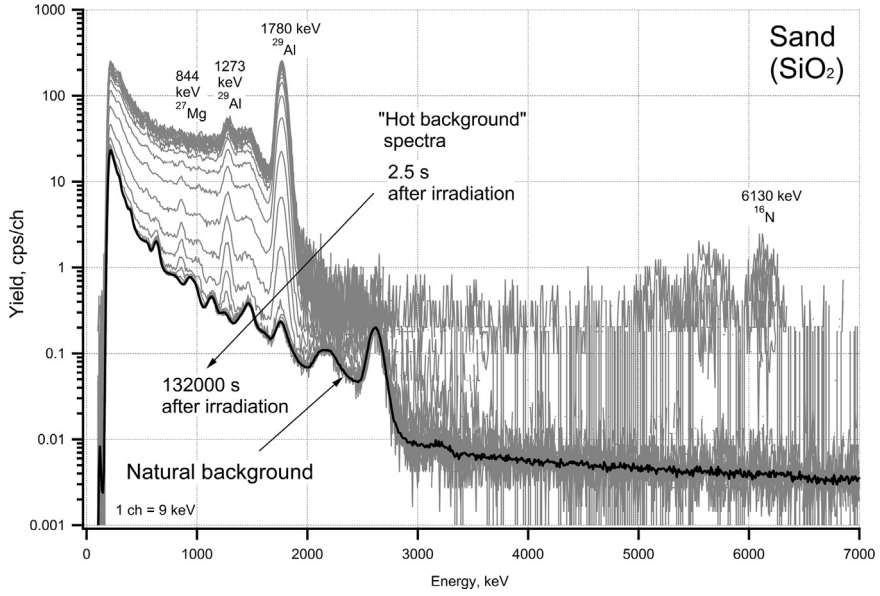

Fig. 7. Sand "hot background" spectra for different times following neutron irradiation, and the natural background spectrum. Main isotopes associated with some peaks are shown near the peaks.

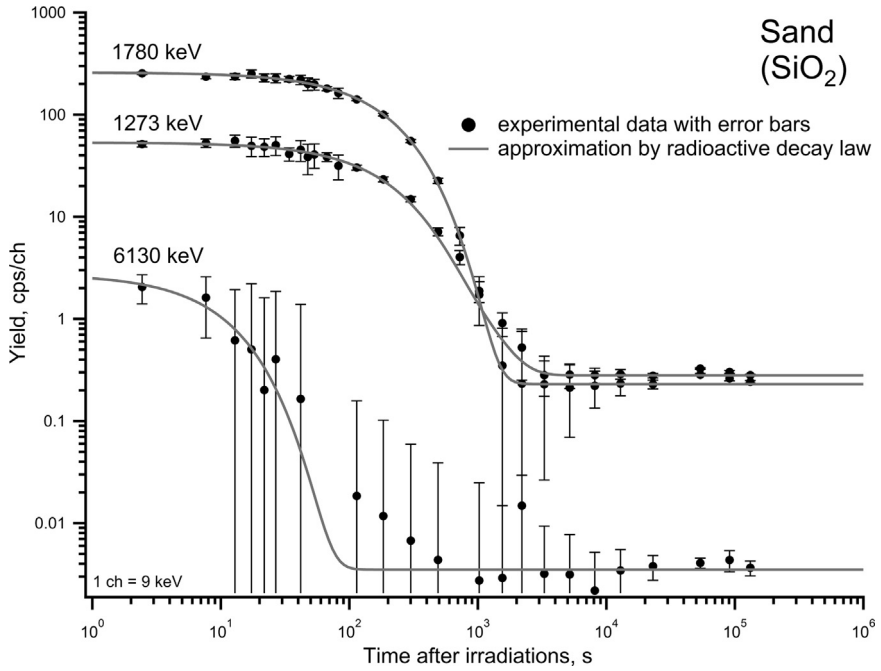

Fig. 8. Time dependencies of peaks in the sand "hot background" spectra. Peak centroid positions are shown for each curve.

$^{27}Al(n_{thermal})^{28}Al$ and $^{56}Fe(n,p)^{56}Mn$ can produce these isotopes in the aluminum and iron parts of the detector. The small peaks that occur around 440 and 1636 keV can be attributed to ^{23}Ne appearing in the detector's body due to the $^{23}Na(n,p)^{23}Ne$ reaction. However, the low intensities of the above mentioned peaks are negligible.

3.6. Neutron generator "hot background"

The MP320 neutron generator consists of an accelerator head and electronics box. The main materials in the accelerator head are: 3020 g of aluminum (housing and end caps), 26 g of copper (tube target base), a 17 g ion source (SS304), a 112 g magnet (rare earth magnet containing Nd, Fe, B), 94 g of acrylic material, 73 g of ceramic material, 166 g of iron, and 17 g of sulfur hexafluoride. The electronics box is composed of carbon steel (~3 mm thick) with an aluminum base plate (~6 mm thick). Inside are two printed circuit boards, wiring, and switches.

All of these components are subjected to neutron irradiation during generator operation. For "hot background" activation, the generator was allowed to run for one hour. Afterwards, the generator was moved to a non-irradiated area and the "hot background" spectra was acquired over several days using a non-irradiated NaI(Tl) gamma detector (Fig. 11). Many features common to the aluminum "hot background" spectra can be seen here. Peaks with centroids at 844, 1014, 1368, 2754, and 4122 keV are found in both spectra. It should be noted that the peak with a centroid at 1780 keV in the neutron generator spectra is relatively other peaks in spectra much higher than that found in the aluminum "hot background" spectra. This can happen if the isotope ^{28}Al (^{28}Al decay is accompanied by 1780 keV gamma quantum) appears due to a process other than thermal neutron capture, since the neutron generator does not have parts that can serve as a moderator. For instance, ^{28}Al can appears due to deuterons reacting with aluminum ($^{27}Al(d,p)^{28}Al$) inside the neutron generator (Al (50 wt%) in the ceramic vacuum envelope can react with deuterons).

Time dependencies of count rates for the above listed energies and their approximations by the radioactive decay law are shown in Fig. 12. The peaks positions and their time constants are the basis for identifying the isotopes responsible for these peaks. Peaks positions in the neutron generator's "hot background" spectra, term number and fitting time constants, isotopes and processes responsible for the peaks, and possible nuclear reactions of isotopes produced are listed in Table 5. Based on these data, it is possible to conclude that the main activation processes within the

Table 4
Positions and decreasing time constants of peaks in the sand (SiO_2) "hot background" spectra, isotope and processes responsible for the peaks, and nuclear reaction producing the isotope.

Peak centroid, keV	Time dependent fitting parameters		Isotope and $T_{1/2}$	Nuclear reaction producing the isotope	Process responsible for the peak
	Term #	Time constant, s^{-1}			
1273	1	$1.76 \cdot 10^{-3}$	^{29}Al 6.56 m	$^{29}Si(n,p)^{29}Al$	$^{29}Al(\beta^-)^{29}Si^* \rightarrow {}^{29}Si+\gamma$
	2	$5.16 \cdot 10^{-3}$	^{28}Al 2.28 m	$^{28}Si(n,p)^{28}Al$	CS from 1780 keV
1780	1	$5.16 \cdot 10^{-3}$	^{28}Al 2.28 m	$^{28}Si(n,p)^{28}Al$	$^{28}Al(\beta^-)^{28}Si^* \rightarrow {}^{28}Si+\gamma$
6130	1	$9.72 \cdot 10^{-2}$	^{16}N 7.13 s	$^{16}O(n,p)^{16}N$	$^{16}N(\beta^-)^{16}O^* \rightarrow {}^{16}O+\gamma$

CS = Compton Scattering.

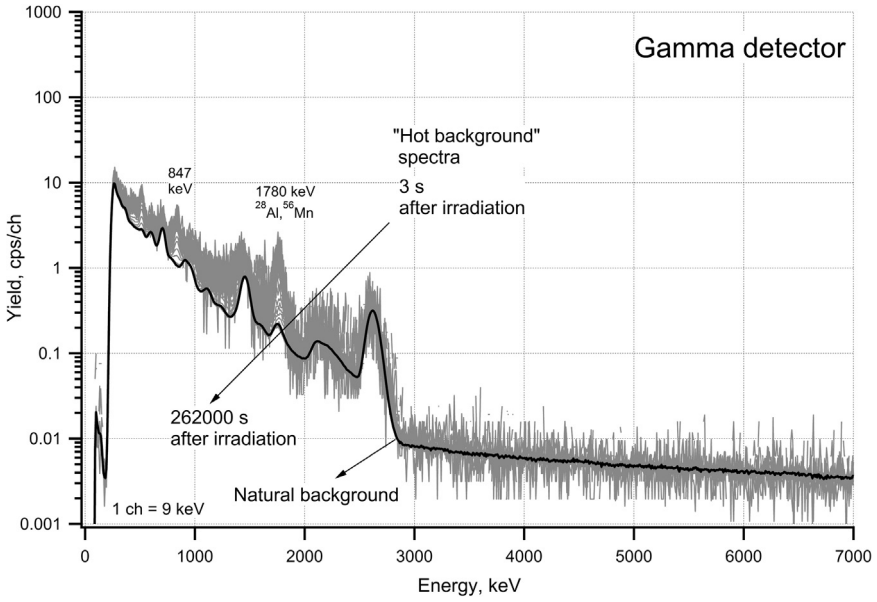

Fig. 9. Detector "hot background" spectra for different times following neutron irradiation, and the natural background spectrum.

neutron generator occur due to aluminum and iron (outer aluminum tube, ceramic vacuum envelope, and inner steel tube). Gamma lines from the neutron generator's "hot background" spectra should be taken into account when analyzing MINS measurements.

3.7. *"Hot background" of MINS system*

The MINS system for soil carbon analysis has been described in detail by Yakubova et al. (2014). The system consists of three separate construction blocks. The first block contains a MP320 neutron generator (Thermo Fisher Scientific, Colorado Springs, CO), a R2D-410 neutron detector (Bridgeport Instruments, LLC, Austin, TX), and the power system. The MINS power system consisted of four DC105-12 batteries (12 V, 105Ah), a DC–AC Inverter (CGL 600 W-series; Nova Electric, Bergenfield, NJ), and a Quad Pro Charger model PS4 (PRO Charging Systems, LLC, LaVergne, TN). This block also contains water, iron and boric acid shielding to decrease system noise (i.e., system background spectra) and to collimate the neutron beam to the area of primary interest. The second block consists of gamma-ray measuring equipment and contains three 12.7 cm × 12.7 cm × 15.2 cm NaI(Tl) scintillation detectors (Scionix USA, Orlando, FL) with corresponding XIA LLC electronics (XIA LLC, Hayward, CA). The third block is a laptop computer which controls the neutron generator, detectors, and data acquisition (ProSpect 0.1, XIA LLC, Hayward, CA). The system is mounted on a mobile platform constructed primarily of aluminum.

Neutrons from the neutron generator irradiate soil underneath the system and all components of the MINS system. The neutron

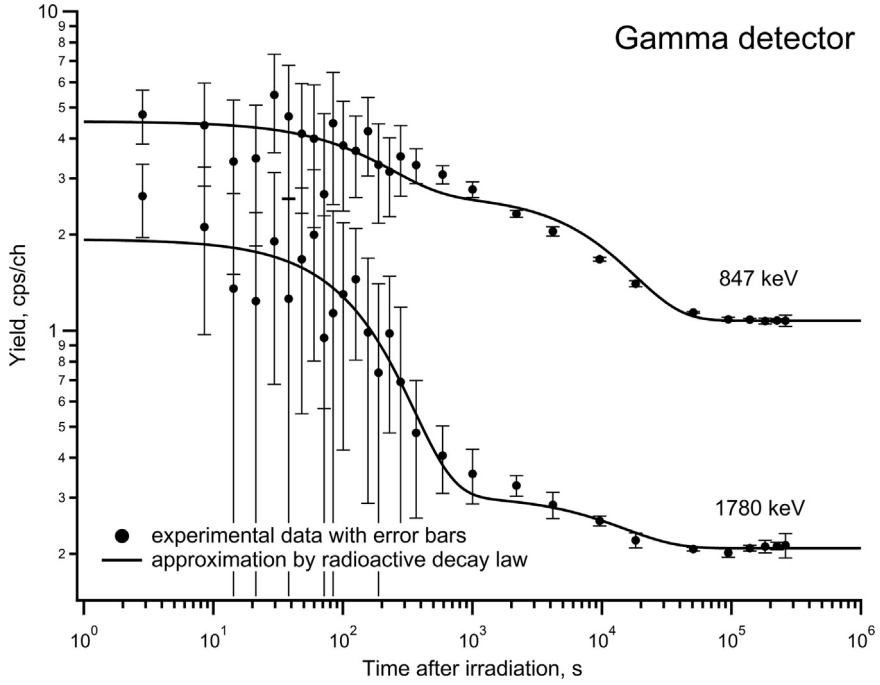

Fig. 10. Time dependencies of peaks in the NaI(Tl) detector "hot background" spectra. Peak centroid positions are shown for each curve.

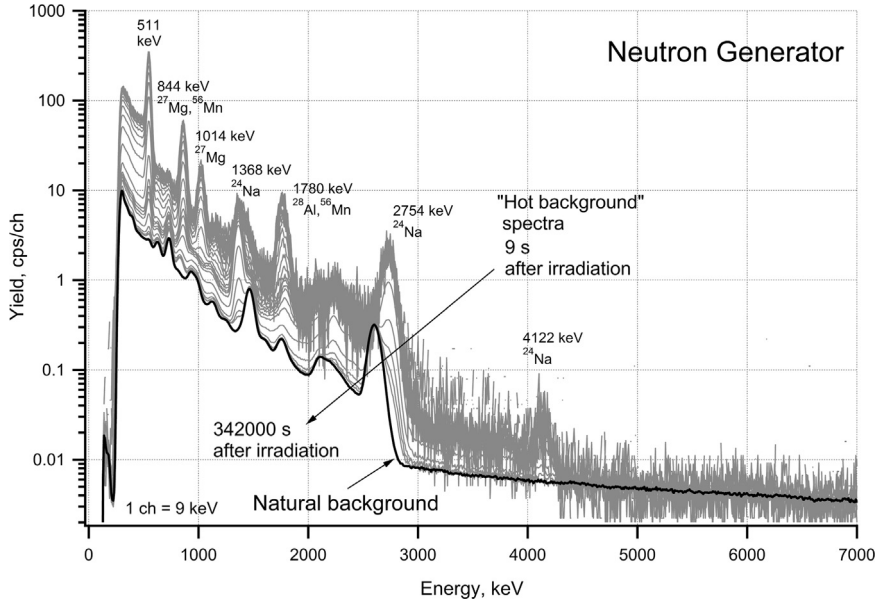

Fig. 11. Neutron generator "hot background" spectra for different times following neutron irradiation, and the natural background spectrum. Main isotopes associated with some peaks are shown near the peaks.

generator body, shielding, batteries, and detail of the frame are under the strongest irradiation, while irradiation of the gamma detectors is much less. Measurement of the MINS system "hot background" and estimations of the effects on both the MINS inelastic neutron scattering (INS) and thermal neutron capture (TNC) spectra were conducted. Measurements of the "hot background" spectra were carried out by MINS system detector and a "cold" (non-irradiated) detector placed in the first block immediately after irradiation. Measurements of the MINS system "hot background" by the system detector were done in two cases, when MINS system was removed from the irradiation location, and when left in the place of irradiation.

The measured MINS system "hot background" spectra are shown in Figs. 13–16. The "hot background" measured by the "cold" detector inside of first system block is shown in Fig. 13. A comparison of these spectra with the neutron generator "hot background" spectra (Fig. 12) showed these to be nearly identical. The time dependence behavior of these spectral peaks is similar to the corresponding peaks in the neutron generator "hot background". Only three additional peaks (strongest peak at 6130 keV) noted in the MINS system "hot background". These peaks can be associated with oxygen contained in the water and boric acid shielding (i.e., $^{16}O(n,p)^{16}N$ nuclear reaction). The time dependence behavior of these spectral peaks is similar to related peaks in the neutron generator "hot background".

The MINS system "hot background" spectra measured by the system detector are shown in Fig. 14 (system removed from place of irradiation) and 15 (system in place of irradiation). The gamma spectra measured during irradiation (INS and TNC spectra) are shown in these plots for comparison. The INS gamma spectra

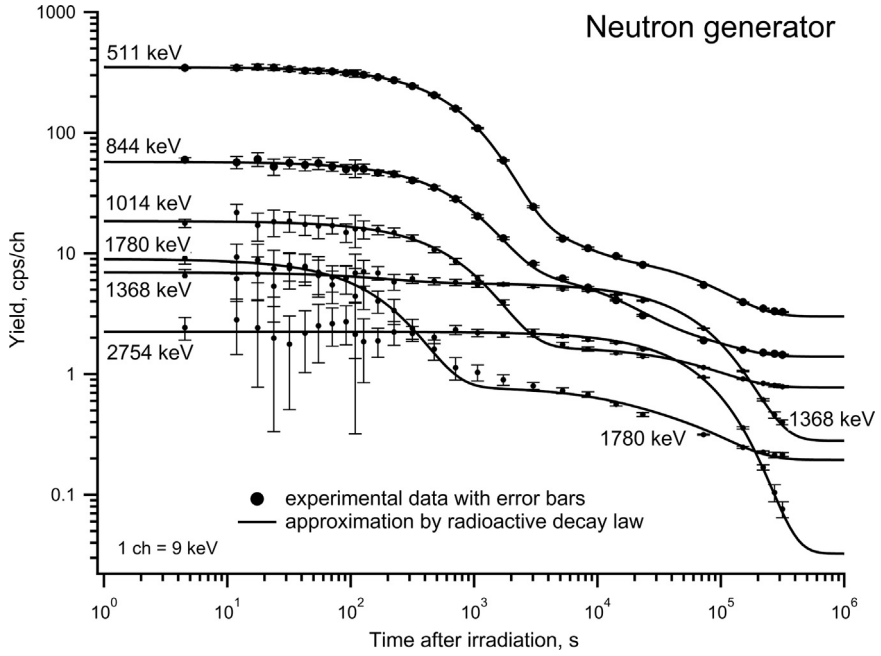

Fig. 12. Time dependencies of peaks in the neutron generator "hot background" spectra. Peak centroid positions are shown for each curve.

Table 5
Positions and decreasing time constants of peaks in the neutron generator's "hot background" spectra, isotope and processes responsible for the peaks, and nuclear reaction producing the isotope.

Peak centroid, keV	Time dependent fitting parameters		Isotope and $T_{1/2}$	Nuclear reaction producing the isotope	Process responsible for peak
	Term # (overlapping peak centroid, keV)	Time constant, s^{-1}			
511	1	$1.22 \cdot 10^{-3}$	Unidentified		
	2	$2.30 \cdot 10^{-4}$	Unidentified		
	3	$1.28 \cdot 10^{-5}$	^{24}Na, 15.0 h	^{27}Al(n,α)^{24}Na	Pair production peak of ^{24}Na gamma rays
844	1 (844)	$1.22 \cdot 10^{-3}$	^{27}Mg, 9.46 m	^{27}Al(n,p)^{27}Mg	^{27}Mg(β$^-$)^{27}Al*→^{27}Al+γ
	2 (847)	$7.54 \cdot 10^{-5}$	^{56}Mn, 2.57 h	^{56}Fe(n,p)^{56}Mn	^{56}Mn(β$^-$)^{56}Fe*→^{56}Fe+γ
	3	$1.28 \cdot 10^{-5}$	^{24}Na, 15.0 h	^{27}Al(n,α)^{24}Na	CS from 1368 keV
1014	1	$1.22 \cdot 10^{-3}$	^{27}Mg, 9.46 m	^{27}Al(n,p)^{27}Mg	^{27}Mg(β$^-$)^{27}Al*→^{27}Al+γ
	2	$1.28 \cdot 10^{-5}$	^{24}Na, 15.0 h	^{27}Al(n,α)^{24}Na	CS from 1368 keV
1368	1	$1.28 \cdot 10^{-5}$	^{24}Na, 15.0 h	^{27}Al(n,α)^{24}Na	^{24}Na(β$^-$)^{24}Mg*→^{24}Mg+γ
	2	$5.16 \cdot 10^{-3}$	^{28}Al, 2.28 m	^{27}Al(d,p)^{28}Al[a]	CS from 1780 keV
1780	1 (1780)	$5.16 \cdot 10^{-3}$	^{28}Al, 2.28 m	^{27}Al(d,p)^{28}Al[a]	^{28}Al(β$^-$)^{28}Si*→^{28}Si+ γ
	2 (1810)	$7.54 \cdot 10^{-5}$	^{56}Mn, 2.57 h	^{56}Fe(n,p)^{56}Mn	^{56}Mn(β$^-$)^{56}Fe*→^{56}Fe+γ
	3 (1732)	$1.28 \cdot 10^{-5}$	^{24}Na, 15.0 h	^{27}Al(n,α)^{24}Na	CS, DE from 2754 keV
2754	1	$1.28 \cdot 10^{-5}$	^{24}Na, 15.0 h	^{27}Al(n,α)^{24}Na	^{24}Na(β$^-$)^{24}Mg*→^{24}Mg+γ
4122	Unidentified		^{24}Na, 15.0 h	^{27}Al(n,α)^{24}Na	Coincidence 1368+2754 keV

CS=Compton Scattering; DE=double escape.

[a] Reaction occurs inside the neutron generator.

consist of gamma lines produced by INS, TNC, delay activation (DA; first spectrum in "hot background" series) and natural background (NB). The TNC gamma spectra consist of the same components, excluding gamma lines due to INS. The DA spectra is the sum of gamma lines due to DA and NB. As can be seen in Figs. 14 and 15, gamma spectra intensities are ranked as follows: INS ≫ TNC ≥ DA ≥ NB. All spectra contain contributions from both the measured object and the MINS system. The TNC spectrum that was measured at the place of irradiation (Fig. 15) coincides with the DA spectra in the energy range near the peak with a centroid of 1780 keV, however there is more than DA spectra in this range when measured in a non-irradiated area (Fig. 14).

The experimental time dependencies of the peak with a centroid of 1780 keV in the MINS "hot background" spectra (in and out of the irradiated area) are shown in Fig. 16 as point symbols with error bars. These dependencies were approximated by radioactive decay law with two exponential terms. The first term shows that the main part of the time peak decreases with a time constant of 0.00516 s^{-1} (2.28 min), and this part of the 1780 keV peak can be attributed to ^{28}Al decay. The second term that is present in both cases at the same low intensity (half-life 35 min) originates from the MINS system, but its origin was not identified.

The ^{27}Al(d,p)^{28}Al reaction yields ^{28}Al inside the neutron generator; ^{28}Al produces 1780 keV radiation that can partially penetrate the shielding. Additionally, the ^{27}Al(n_{therm})^{28}Al reaction can happen in the aluminum frame of the MINS platform (i.e., thermal neutrons appear due to moderation in water and boric acid shielding). At the irradiated site, the ^{28}Al isotope also was activated in soil due to the ^{28}Si(n,p)^{28}Al reaction. Thus, the 1780 keV peak in the DA spectra out of the irradiation area appears due to MINS system activation only, and an additional portion of the peak in the irradiation area is due to soil activation.

The DA spectrum that was measured at the place of irradiation coincides with the TNC spectra energy range near the peak with a centroid of 1780 keV. This experimentally supports the earlier theoretical analysis of Wielopolski (2011) regarding the origin

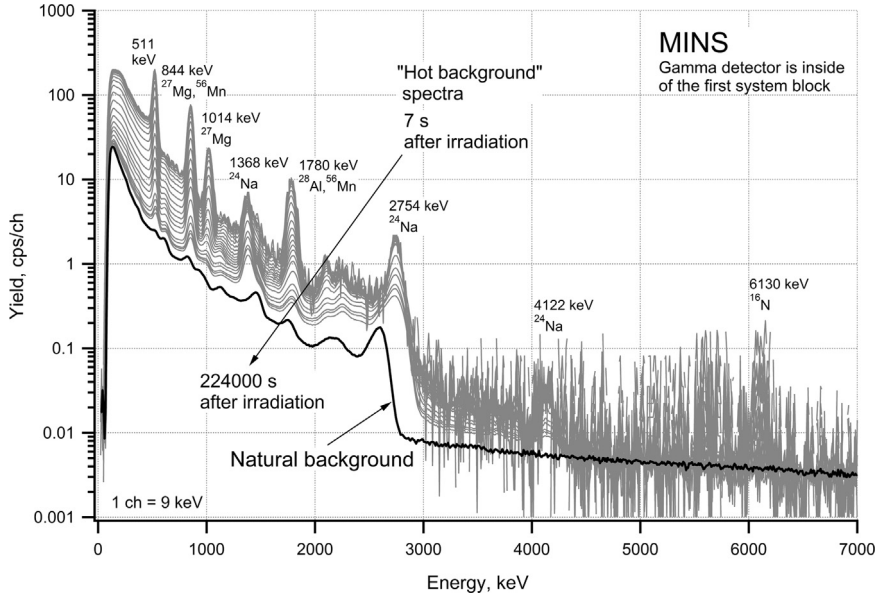

Fig. 13. MINS system "hot background" spectra for different times following neutron irradiation (measured inside the first block of the MINS system, see text) and the natural background spectrum. Main isotopes associated with some peaks are shown near the peaks.

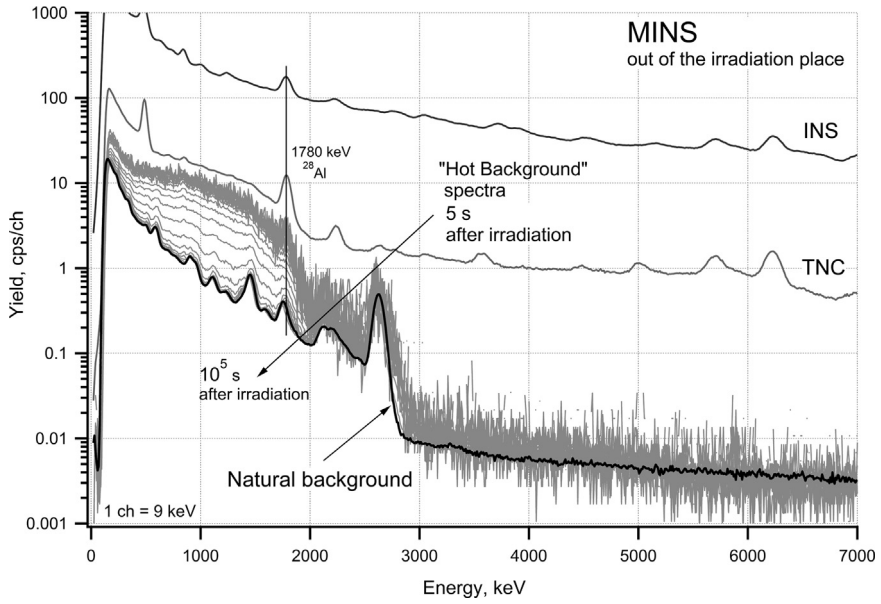

Fig. 14. The MINS system "hot background" spectra measured by system detector (system removed from the area of irradiation). Main isotopes associated with 1780 keV peak are shown near the peak.

(^{28}Al decay) of the 1780 keV peak in the TNC soil spectra.

The peak area with a centroid at 1780 keV in the TNC spectra is used when determining the carbon corrected peak area in MINS soil carbon measurements (Wielopolski, 2011). However, due to presence of two inputs (from sample and measurement system) to this peak, the equation given in Wielopolski (2011) for carbon corrected peak area calculation should be refined.

4. Conclusion

The time dependent behavior of the gamma spectra from the 14 MeV neutron activated materials (Al, Si, SiO_2, Fe), neutron generator, NaI(Tl) gamma detector, and MINS (whole system), was studied in the interest refining soil carbon determination by the inelastic neutron scattering method. The identification of activated isotopes and possible nuclear reactions that govern their appearance was made on the basis of peak positions and decay time constants. In particular, it was demonstrated that self-irradiation of the neutron generator activates ^{27}Mg and ^{24}Na isotopes in the aluminum housing, but ^{28}Al appears due to deuteron interaction with ceramic in the vacuum envelope of the neutron generator. Silicon, sand, and soil neutron irradiation causes activation of the ^{28}Al isotope. Decay of this isotope is responsible for the dominant gamma peak with a centroid at 1780 keV. This delay activated gamma line from soil samples appears in the soil TNC spectra as the first component. The second main component in this peak is the gamma line from the ^{28}Al isotope activated by self-irradiation of the MINS system. This double component peak (from soil and the measurement system) in the soil TNC spectra should be accounted for when calculating the carbon corrected peak area in soil carbon neutron gamma analysis. To do so, the MINS system

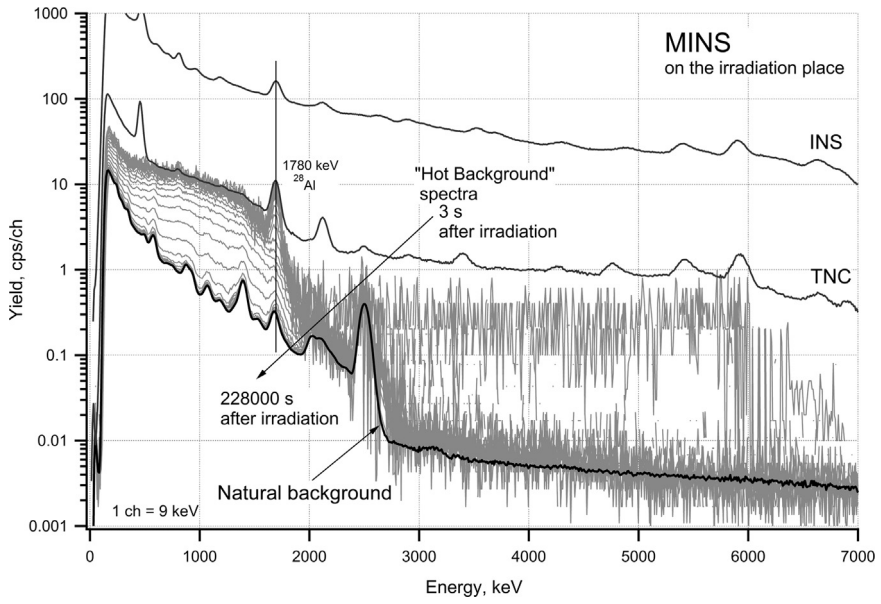

Fig. 15. The MINS system "hot background" spectra measured by system detector in the area of irradiation. Main isotopes associated with 1780 keV peak are shown near the peak.

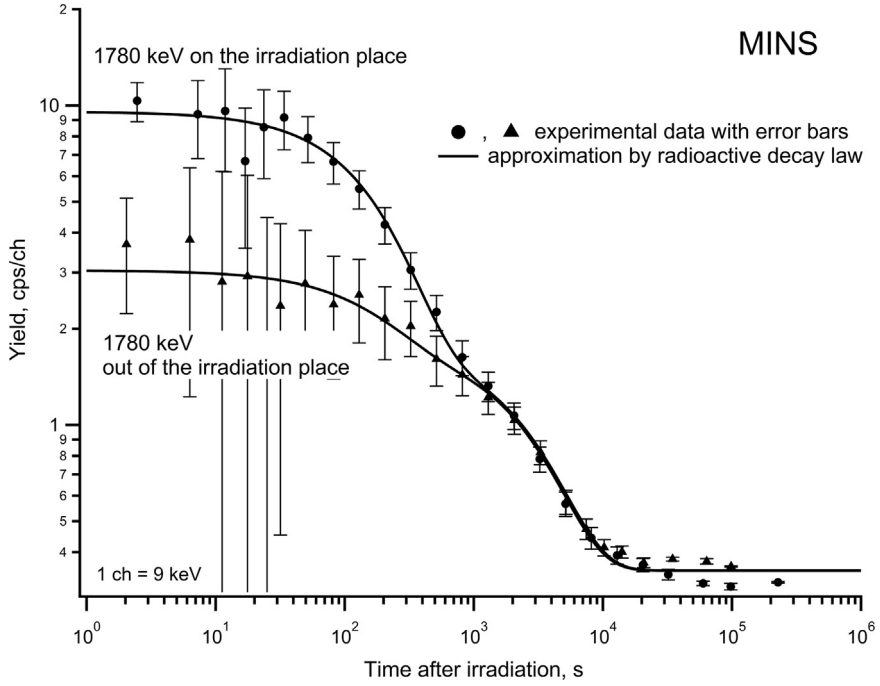

Fig. 16. Time dependencies of the peak with a centroid at 1780 keV in the MINS "hot background spectra" measured in and out of the irradiation area.

Table 6
Isotopes occurring in materials and parts of the MINS system when activated by 14 MeV neutrons.

Isotope	Half-life	Decay time constant, s^{-1}	Energy of gamma lines, keV	Producing reaction	Material or system part
^{28}Al	2.28 m	$5.16 \cdot 10^{-3}$	1780	^{27}Al($n_{thermal}$)^{28}Al ^{28}Si(n,p)^{28}Al ^{27}Al(d,p)^{28}Al	Si, SiO_2, Al, Detector, Neutron Generator
^{56}Mn	2.58 h	$7.54 \cdot 10^{-5}$	847 1810 2113	^{56}Fe(n,p)^{56}Mn	Fe, MINS system
^{27}Mg	9.46 m	$1.22 \cdot 10^{-3}$	844 1014	^{27}Al(n,p)^{27}Mg ^{30}Si30(n,α)^{27}Mg	Al, Si, SiO_2, MINS system
^{24}Na	14.99 h	$1.28 \cdot 10^{-5}$	1368 2754 4122	^{27}Al(n,α)^{24}Na	Al, MINS system
^{23}Ne	37 s	$1.86 \cdot 10^{-2}$	440 1636	^{23}Na(n,p)^{23}Ne	NaI detector
^{16}N	7.13 s	$9.7 \cdot 10^{-2}$	6130 5620 5110	^{16}O(n,p)^{16}N	SiO_2, MINS system
^{29}Al	6.56 m	$1.76 \cdot 10^{-3}$	1273	^{29}Si(n,p)^{29}Al	Si, SiO_2

component is a background component that should be measured and extracted during calculations (details of this procedure can be found in Yakubova et al., 2015).

Table 6 lists isotopes occurring in soil, construction materials, and other parts of the MINS system that are activated by 14 MeV neutrons; their half-lives and decay time constants, main gamma line energies, and possible nuclear reactions are also shown. The presented data should be used in identifying gamma spectrum peaks that appear when conducting soil carbon (and other soil elements) analysis using the mobile inelastic neutron scattering (MINS) system.

Acknowledgments

The authors are indebted to Barry G. Dorman, Robert A. Icenogle, Marlin R. Siegford, and Morris G. Welch for technical assistance in experimental preparation. We thank XIA LLC for allowing the use of their electronics and detectors in this project.

References

Frank, V., Tolgyessy, J., 1993. The chemistry of soil. In: Tolgyessy (Ed.), Chemistry and Biology of Water, Air and Soil Environmental Aspects. Elsevier, United States, ISBN 13: 978-0-444–98798-3.

NNDC, 2012. Brookhaven National Laboratory, Upton, NY. Available at: ⟨http://www.nndc.bnl.gov/chart⟩.

Turner, J.E., 2007. Atoms, Radiation, and Radiation Protection. WILEY-VCH Verlag GmbH & Co. KGaA, Weinheim.

WaveMetrics, 2013. IGOR Pro. ⟨http://www.wavemetrics.com/products/igorpro/igorpro.htm⟩.

Wielopolski, L., 2011. Nuclear methodology for non-destructive multi-elemental analysis of large volumes of soil. In: Carayannis, E. (Ed.), Planet Earth: Global Warming Challenges and Opportunities for Policy and Practice, ISBN: 978-953-307–733-8.

Wielopolski, L., Song, Z., Orion, I., Hanson, A.L., Hendrey, G., 2005. Basic considerations for Monte Carlo calculations in soil. Appl. Radiat. Isot. 62, 97–107.

Wielopolski, L., et al., 2004. Non-Destructive Soil Carbon Analyzer (ND-SCA), Formal report, BNL-72200-2004. Available at ⟨https://www.bnl.gov/isd/documents/26295.pdf⟩.

Wolfram Research, Inc., 2013. Champaign, IL. Available at: ⟨http://periodictable.com/Properties/A/IsotopeAbundances.html⟩.

Yakubova, G., Kavetskiy, A., Prior, S.A., Torbert, H.A., 2015. Benchmarking the inelastic neutron scattering soil carbon method. Vadose Zone J. . http://dx.doi.org/10.2136/vzj2015.04.0056

Yakubova, G., Wielopolski, L., Kavetskiy, A., Torbert, H.A., Prior, S.A., 2014. Field testing a mobile inelastic neutron scattering system to measure soil carbon. Soil Sci. 179, 529–535.